Environmental Pollution 236 (2018) 992–1003

Contents lists available at ScienceDirect

Environmental Pollution

journal homepage: www.elsevier.com/locate/envpol

Physiochemical characteristics of aerosol particles collected from the Jokhang Temple indoors and the implication to human exposure☆

Lulu Cui [a], Bu Duo [a, d], Fei Zhang [a], Chunlin Li [a], Hongbo Fu [a, b, c], Jianmin Chen [a, *]

[a] Shanghai Key Laboratory of Atmospheric Particle Pollution and Prevention, Department of Environmental Science & Engineering, Institute of Atmospheric Sciences, Fudan University, Shanghai, 200433, China
[b] Shanghai Institute of Pollution Control and Ecological Security, Shanghai, 200092, China
[c] Collaborative Innovation Center of Atmospheric Environment and Equipment Technology(CICAEET), Nanjing University of Information Science and Technology, Nanjing, 210044, China
[d] Department of Chemistry& Environmental Science, Tibet University, Lhasa 850000, China

ARTICLE INFO

Article history:
Received 18 July 2017
Received in revised form
24 October 2017
Accepted 24 October 2017
Available online 13 February 2018

Keywords:
Indoor air pollution
PAHs
Benzo(a)pyrene
health risk
Carcinogenic metals
Tibet Plateau

ABSTRACT

This paper presents a detailed study on the indoor air pollution in the Jokahng Temple at Tibet Plateau, and its implication to human health. The mean concentrations of $PM_{1.0}$ and $PM_{2.5}$ were 435.0 ± 309.5 and 483.0 ± 284.9 μg/m^3, respectively. The $PM_{2.5}$ concentration exceeded the National Ambient Air Quality Standard (75 μg/m^3) by 6.4 times. The size-segregated aerosols displayed a bimodal distribution. One peak was observed in the fine mode (0.4–2.1 μm) and the other peak appeared in the coarse mode (2.1–9.0 μm). The concentration of the total size-resolved PM was 794.3 ± 84.9 μg/m^3. The mass fraction of coarse particles shared by 41.1%, apparently higher than that reported at low altitudes, probably due to incomplete combustion at Tibet Plateau with hypoxic atmospheric environment. The total concentration of polycyclic aromatic hydrocarbons (PAHs) was 331.2 ± 60.3 ng/m^3, in which the concentration of benzo(a)pyrene (BaP) was 18.5 ± 4.3 ng/m^3, over ten times higher than the maximum permissible risk value of 1 ng/m^3 on account of carcinogenic potency of particulate PAHs through inhalation. PAHs exhibited a trimodal distribution, of which two peaks were observed in the fine mode and one peak in the coarse mode. With the aromatic rings increasing, the peak intensity increased in the fine mode. Na, Ca, Al, Mg and K dominated the elemental mass profiles, and metals displayed a bimodal distribution with a dominant peak in the coarse range. The total PAH deposition flux was 123.6 and 53.1 ng/h for adults and children, respectively. Coarse particles contributed most deposition flux in the head region, while fine particles contribute most deposition flux in the alveolar region. The increment lifetime cancer risk (ILCR) of PAHs ranaged at 10^{-5}-10^{-4}, indicating potential cancer risk to human health. The total deposition flux of metals was estimated at 1.4–13.2 ng/h. With the size increasing, deposition flux increased in the head region while decreased in the alveolar region. The highest ILCR of Cr and Ni were 4.9×10^{-5} and 1.5×10^{-6}, respectively, exceeding the permissible risk of 10^{-6}. The hazard quotient (HQ) of Fe (10^{-5}-10^{-4}) and Zn (10^{-6}-10^{-5}) were much lower than the safe level of 1.0, and thus they were not considered as a health concern.

1. Introduction

Indoor air quality (IAQ) has been focused as a hotspot field during the past years due to the fact that people spend most of their lifetime indoors (Schweizer et al., 2007; Rebecca et al., 2013; Hussein, 2014). Generally, the poor ventilation condition indoors facilitates retention of greater amount of air pollutants (Beko et al., 2013; Wierzbicka et al., 2015). The indoor air pollution could derive from a series of human activities, concluding walking, incense burning, cooking, tobacco smoking, and electrical appliances, etc (Jones, 1999; Wang et al., 2006; Karimatu et al., 2013). The pollutants emitted from human activities, especially the fine mode particles are prone to depositing in human respiratory system, and thus could cause adversr effects to human health, such as

☆ This paper has been recommended for acceptance by Eddy Y. Zeng.

* Corresponding author. Shanghai Key Laboratory of Atmospheric Particle Pollution and Prevention, Department of Environmental Science & Engineering, Institute of Atmospheric Science, Fudan University, Shanghai 200433, China.
E-mail address: jmchen@fudan.edu.cn (J. Chen).

https://doi.org/10.1016/j.envpol.2017.10.107
0269-7491/

inflammatory responses, and cardiopulmonary diseases (Bitterle et al., 2006; Kawanaka et al., 2004; Li et al., 2017a,b).

In many Asian countries with religious beliefs, incense burning is a common source of indoor air pollution. The raw material of incense generally constitutes various fragrant plant substances concluding flowers, resin, essential oils, tree bark, and spices (Jetter et al., 2002). Due to the complex mixture of ingredients, the emission factors of particles from incense burning could be much higher than those from combustion of charcoal, wood, and cigarette (Shih-Chun et al., 2006; Oanh et al., 1999; Rebecca et al., 2013). The temple is a special indoor public venue where incense is frequently burned for religious rites and festivals. The confined space, relatively dense flow of people, and poor ventilation could lead to severe indoor air pollution (Shih-Chun et al., 2003). An assessment on the incense particles revealed that the concentration of total suspended particles (TSP) was about 11 times higher than that outside the temple (Lin et al., 2001). Lung and Kao (2003) further found that burning incense in the Buddhist temples generated massive quantities of fine particles (aerodynamic diameter < 2.5 mm: $PM_{2.5}$), which were markedly higher by 10–20 times than the indoor air quality standard of Taiwan (35 μg/m^3).

The particles emitted from incense burning could host a wide range of toxic components, including metals, inorganic ions, PAHs, carbonyl compounds, etc., all of which could deteriorate IAQ and bring health risk (Rasmussen, 1987; Kuo et al., 2008; Wang et al., 2007; Tsai et al., 2010). Kuo and Tsai, (2017) found allergenic terpenols in the emissions from the Taiwanese and Thai incense burning, which could increase the contact dermatitis, bronchoconstriction, asthma and chronic obstructive pulmonary disease (Matura et al., 2002; Weschler, 2006). Besides, high levels of PAHs were frequently observed from incense burning, which were mainly hosted by fine and ultrafine particles (Lin et al., 2002; Chen et al., 2005). Certain PAHs could retain for a long time in human tissue due to their high lipophilicity (Newman, 2010), and thus exert the adverse effects to human health such as the DNA damage and lung inflammation (Heinrich et al., 1994). Furthermore, metallic components within raw material of incenses also have a health concern, even though they just constitute a small fraction of the particles. Hazardous metals such as Cd, Mn, Cr, Ni, Fe, Zn, and Pb were commonly observed as the emissions of incense burning, all of which could be immediately internalized and pose potentially health risk such as cellular pro-inflammatory response (Adamson et al., 2000; Fang et al., 2013; Majestic et al., 2007). However, previous studies mainly focused on characterizing the emission of chemical constitutes in mere fine particles, the particle size distribution of chemical species associated with human health effects is presently poorly known (Lin et al., 2002; Fang et al., 2003, 2009; Chiang et al., 2009; Rebecca et al., 2013).

Lhasa, which is well known as the holy land of Tibetan Buddhism, has an area of about 31, 662 square kilometers and 0.5 million of population. Worshipping Buddha with burning incense is a traditional custom of the Tibetan culture. There are 286 temples and more than 4800 monastics at Lhasa (Zheng and Ma, 2013). Given a unique location in the middle of the Tibetan Plateau (TP) with an elevation of 3650 m, the amount of oxygen in Lhasa air is about 60–70% of the normal level (Gong et al., 2011). The more common types of incense applied in the local temples are Liuwu and Sheng Kang (two local brands) incense sticks, which are made mainly from medicinal aromatic plants, sandalwood, eaglewood and pangolin. As Buddhists spend considerable time to worship inside the temples, the air pollution in temple indoors and its implication to human health have become an important concern.

As the most sacred temple of Tibetan Buddhism, the Jokhang Temple was selected as the study site. It is located in downtown Lhasa (shown in Fig. S1) with an area of more than 20,000 square meters. The average number of visitors is nearly 10,000 to 20,000 per day, which is significantly higher than the famous Buddhist-Taoist combined temple at Taiwan (Chiang et al., 2009). A significant amount of incense is burned on a daily basis for the religious purposes. Especially, the application amount of incense increases sharply on specific days (e.g., Saga Dawa Festival, Seance festival and Exorcism festival, and the 3rd, 5th, 8th, 10th, 15th and 30th day of each Tibetan lunar month). The aim of this study is as follows: (1) to determine the physiochemical characteristics of incense burning particles, (2) to compare the data with those observed in temples located at low altitude places, and (3) to quantify the health risks associated with the pollutants exposure inside the Jokhang Temple.

2. Materials and methods

2.1. Sampling description

Sampling work was conducted at the main hall of the Jokhang Temple from 29 to 31 August 2014. The location of the sampling site was illustrated in Fig. S1. An Anderson eight-stage particle separator (Tisch Environmental Inc., USA) was used to collect particles at an inlet flow rate of 28.3 L/min. Particles in the size bins of 5.8–9.0, 4.7–5.8, 3.3–4.7, 2.1–3.3, 1.1–2.1, 0.7–1.1, 0.4–0.7 and < 0.4 μm were collected on quartz fiber filters (Whatman QMA, 47 mm). The filters were baked in the muffle furnace under 400–500 °C, and then equilibrated at a constant temperature (20 °C) and relative humidity (RH, 40%) for 24 h before sampling (Lyu et al., 2016). All of the filters were weighted before and after sampling by a balance (Sartorius BP211D), and each filter was weighed for several times until the difference between two repeated weighing was within ±15 μg. After weighting, the loaded filters were stored in a refrigerator at 20 °C for further analysis.

2.2. Particle mass concentration

The mass concentration of PM was measured by a real-time personal aerosol monitor (AM510 SidePak™). This instrument measures mass concentration of particles based on the light-scattering technology (Morabia et al., 2009). The DustTrak can measure particles with a size range of 0.1–15 μm at the concentration scope of 0.001–150 mg/m^3 (Li et al., 2015). The personal aerosol monitors were equipped with a size-selective inlet for $PM_{2.5}$ or $PM_{1.0}$.

2.3. Chemical analysis

1/4 of each filter was cut down for PAH analysis. The filter was extracted by Soxhlet extraction with 200 mL of acetone/hexane (1:1, v/v) for 22 h, and washed by 1.5 mL of 0.5 M KOH solution and cleaned with 3% of water deactivated alumina (MP Biomedicals GmbH, Eschwege, Germany) for column chromatography after rotary evaporation. Finally, the extracts were concentrated for gas chromatography coupling with mass spectrometry (GC-MS, 7890A-5975C: Agilent, Santa Clara, CA, USA) analysis (Wang et al., 2016). Chemical standards for 12 PAH compounds designated by the United States EPA including naphthalene (NaP), acenaphthene (Ace), acenaphthylene (Acy), Anthracene (Ant), Fluorene (Flu), Fluoranthene (FL), Phenanthrene (Phe), Benzo(a)anthracene (BaA), Benzo(a)pyrene (BaP), Benzo(b)fluoranthene (BbF), Benzo(k)fluoranthene (BkF) and Chrysene (Chry) were acquired from AccuStandard (New Haven, CT, USA) and J&K Chemical (Beijing, China). More detailed QA-QC procedures were described previously (Delgado-Saborit et al., 2009, 2010).

1/4 of each filter was digested by high concentrated acid ($HF:HNO_3:HClO_4$, with a mixture ratio of 3:1:1), and kept at 170 °C

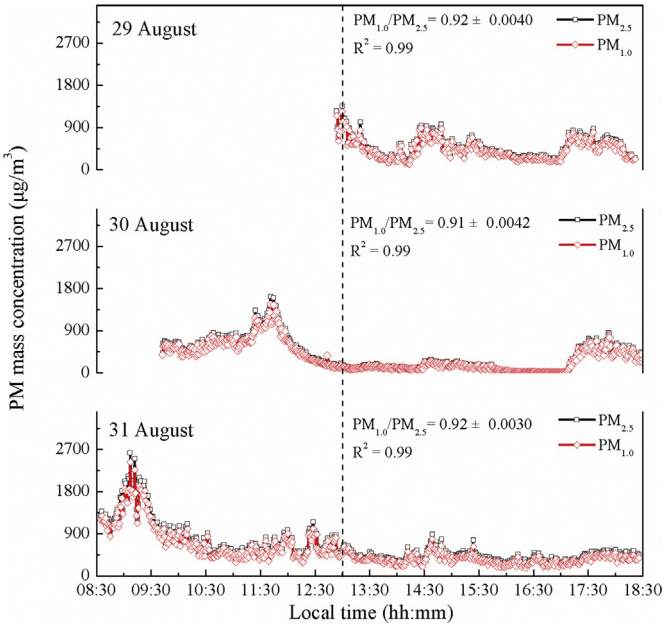

Fig. 1. Temporal variation patterns of fine particle in mass concentration.

for four hours in a closed Teflon digestion vessel. The procedures were repeated several times until the residuals were completely dissolved. Finally, the digestion solution was diluted by ultrapure water into 10 mL for element analysis. Metal elements were analyzed by inductively coupled plasma atomic emission spectrometry (ICP-AES). More detailed description regarding the analytic procedure was published previously (Voutsa et al., 2015). All metals and regents for standard solutions used in the present study were of analytic grade. Filter and procedural blanks, duplicate analysis and standard calibration were conducted for validation of the analytical data.

2.4. Health risk assessment

2.4.1. PAHs health assessment

In order to assess the influence of size-resolved PAHs on human respiratory potential, the deposition efficiency and flux of PAHs was calculated by an International Commission on Radiological Protection (ICRP) model. Based on inhaled particles sizes, the respiratory tract was sorted into three deposition regions: head airway (HA), tracheobronchial region (TR), and alveolar region (AR). The detailed information on calculating with this model was included elsewhere (Lyu et al., 2016; Zhang et al., 2012). The inhalation rate of people is shown in Table S1. The deposition efficiency of size-resolved particles in HA, TR and AR regions was estimated by the following equations:

$$DE_{HA} = IF \times \left[\frac{1}{1+e^{6.84+1.183InDp}} + \frac{1}{1+e^{0.924-1.885InDp}}\right] \quad (1)$$

$$DE_{TB} = \left(\frac{3.52\times10^{-3}}{Dp}\right) \times \left[e^{-0.234(InDp+3.40)^2} + 63.9 \times e^{-0.819(InDp-1.61)^2}\right] \quad (2)$$

$$DE_{AR} = \left(\frac{0.0155}{Dp}\right) \times \left[e^{-0.416(InDp+2.84)^2} + 19.11 \times e^{-0.482(InDp-1.362)^2}\right] \quad (3)$$

Where Dp is the diameter of the particles, IF is the inhalable fraction of the size-resolved particles:

$$IF = 1 - \left(1 - \frac{1}{1+7.6Dp^{2.8}\times10^{-4}}\right)\Big/2 \quad (4)$$

Incremental lifetime cancer risk (ILCR) was calculated to estimate the potential cancer risk of PAHs exposure in the Jokhang Temple. ILCR for pilgrims through inhalation, direct ingestion and dermal contact were calculated using the following carcinogenic risk equation:

$$LADD_{\text{inh}} = \frac{C_a \times IR_a \times RT \times VF \times ED \times cf}{BW \times AT_c} \quad (5)$$

$$LADD_{\text{ing}} = \frac{C_{pa} \times IR_p \times RT \times VF \times ED \times cf}{BW \times AT_c} \quad (6)$$

$$LADD_{\text{ing}} = \frac{C_{pa} \times AB \times \times SA \times EV \times AF_d \times RT \times VF \times ED \times cf}{BW \times AT_c} \quad (7)$$

$$ILCR_i = LADD_i \times (CSF_i) \times \left((BW/70kg)^{1/3}\right) \quad (8)$$

$$TILCR = \sum_i^3 ILCR_i \quad (9)$$

The implications, units and reference values in equations (1)–(5) are listed in Table S1. An ILCR between 10^{-6} and 10^{-4} implies potential risk, whereas that greater than 10^{-4} indicates high potential risk (USEPA, 2001).

2.4.2. Elemental health assessment

The ICRP model was used for evaluating the influence of size-resolved metals on the human respiratory tract. The daily intake by ingestion and dermal contact (US-EPA , 2001) was calculated by the following Eqs. (6) and (7):

$$DI_{ing} = C_{UCL} \times \frac{R_{ing} \times EF \times ED}{BW \times AT} \times CF \quad (10)$$

$$DI_{dermal} = C_{UCL} \times \frac{SAF \times A_{skin} \times DAF \times EF \times ED}{BW \times AT} \times CF \quad (11)$$

In term of inhalation, the following equation adopted from Cheng et al. (2016) was described as follows:

$$DI_{inh} = \frac{C \times IR \times ED}{BW \times AT} \quad (12)$$

The implications, units, and reference values used in Eqs. (6)–(8) are listed in Table S2.

The incremental probability of cancer risk for individual element was calculated as follows:

$$ILCR = DI \times CSF \quad (9)$$

The reference CSF values for Ni and Cr are 0.8 and 42, respectively (Jiang et al., 2016).

The non-carcinogenic risk was calculated by:

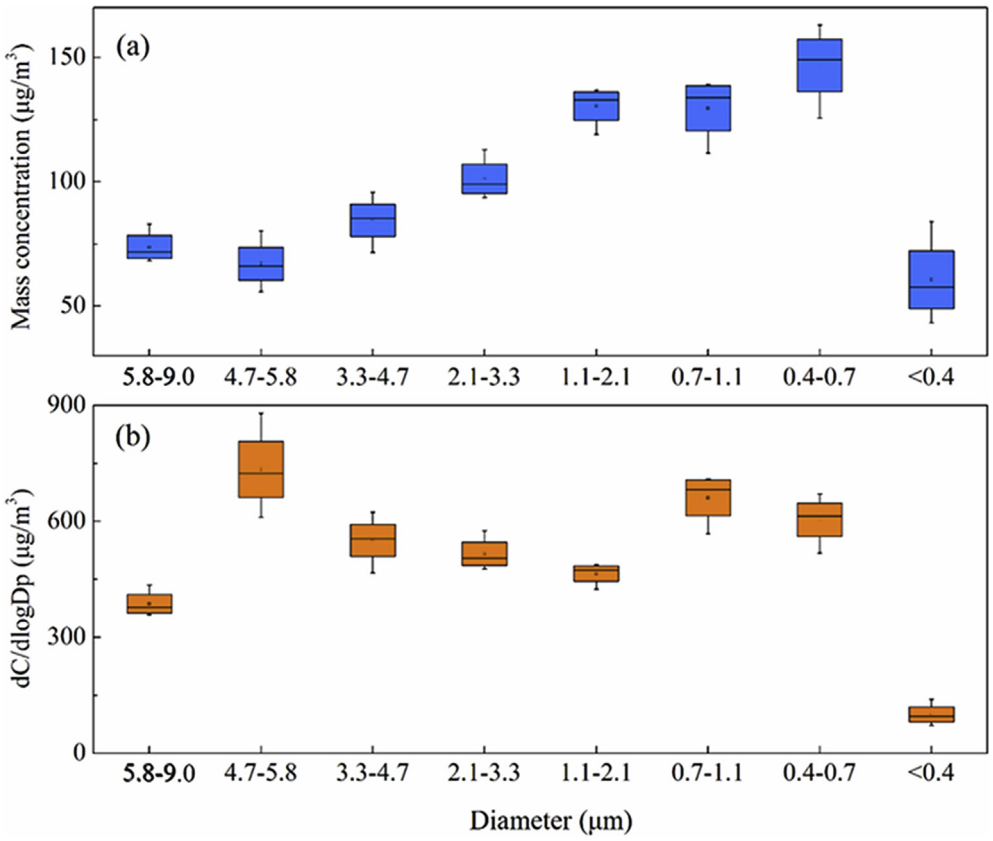

Fig. 2. Box and whisker plots of the PM mass concentrations in the size-resolved particles.

$$HQ = DI/RfD \quad (13)$$

If the hazard quotient of HQ is < 1, the health concern was not considered, for HQ ≥ 1, adverse health effects are possible and more attention should be paid. The reference RfD values of Fe and Zn are 0.7 and 0.3 mg/(kg·d), respectively.

3. Results and discussion

3.1. The concentration of fine particles at the Jokhang Temple indoors

Fig. 1 shows the temporal variations of $PM_{1.0}$ and $PM_{2.5}$ mass concentrations during the sampling. The $PM_{1.0}$ and $PM_{2.5}$ concentrations ranged at 5–2430 and 6–2620 μg/m^3, and averaged at 435.0 ± 309.5 and 483.0 ± 284.9 μg/m^3, respectively. The mass concentration of $PM_{2.5}$ was much higher by 6.4 times than that of the National Ambient Air Quality Standard (75 μg/m^3). It has been demonstrated that each 10 μg/m^3 increase in fine particle mass concentration could raise the death risk from lung cancer by about 8% (Pope, 1999). The exceedance of the daily $PM_{2.5}$ standards in the Jokhang Temple implied a great health concern.

In order to investigate the emission characteristics of the particles in the temple air, the mass concentration ratio of $PM_{1.0}/PM_{2.5}$ was further analyzed. The mean ratios of $PM_{1.0}/PM_{2.5}$ herein were calculated at 0.92. This pattern was in fair agreement with the previous studies, which found that most of the particles displayed aerodynamic diameters below 1 μm (Yang et al., 2007; Jetter et al., 2002; Zhou et al., 2016). Given a significant influence of the finer particles on cardiopulmonary diseases and lung cancer, the information about size distributions of particles is essential to further evaluate the exposure risk of incense burning particles to human body.

3.2. Size-segregated mass concentration and chemical composition of particles

3.2.1. Size-segregated mass distributions

For the size-resolved particles, those smaller than 2.1 μm were labeled as the fine fraction, while those with the diameters of 2.1–9.0 μm were termed as the coarse one. As illustrated in Fig. 2, particle size presented a bimodal distribution with one peak in the

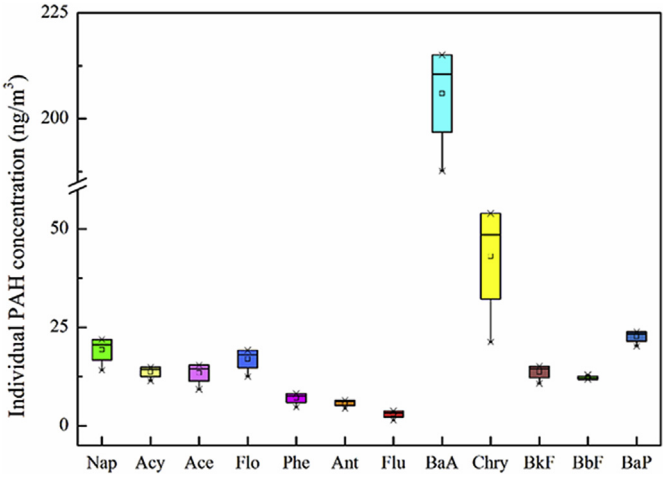

Fig. 3. Box and whisker plots of the individual PAH concentrations.

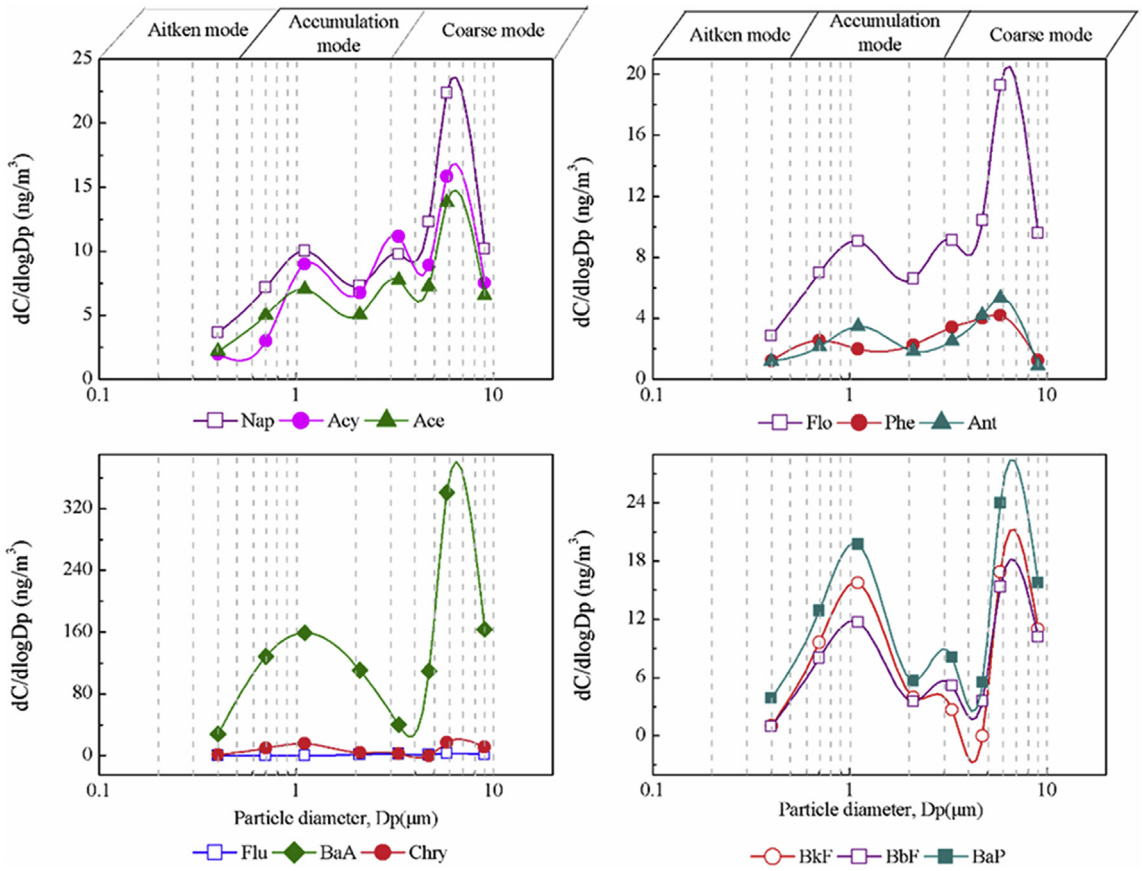

Fig. 4. Particle size distribution of PAHs for all samples. dC is the concentration on each filter, C is the sum concentration on all filters, and dlogDp is the logarithmic size interval for each impactor stage in the aerodynamic diameter (Dp).

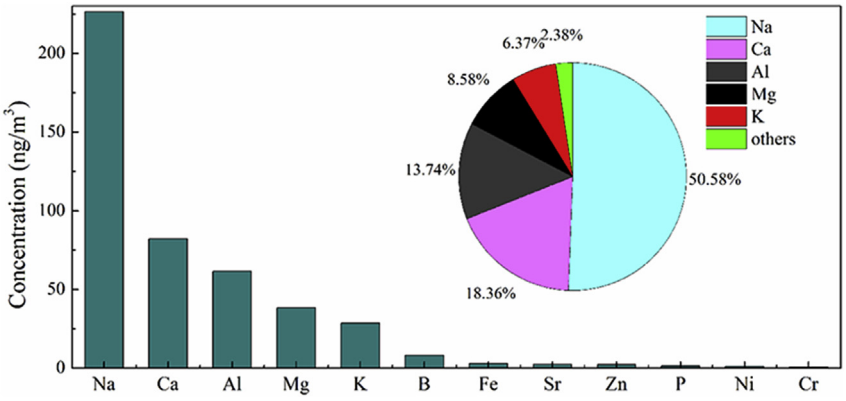

Fig. 5. Concentration profile of metallic elements in PM.

fine size range (0.4–2.1 μm) and the other peak in the coarse size range (2.1–9.0 μm). The fine modal peak indicates direct emission from incense burning, whereas the peak of coarse mode may originate from the contribution of incomplete combustion and/or re-suspended soil dust (Long et al., 2001; Li et al., 2017a,b). The concentration of the total PM was 794.3 ± 84.9 μg/m^3 during the sampling periods. Specifically, the coarse particles constituted 41.1% of the total particles by mass. The mass fraction of the coarse particles was apparently higher as compare to that measured at low latitudes such as Taiwan (30%) and Hongkong (18%) (Fang et al., 2003, 2009; Wang et al., 2007). This implied that the incomplete combustion degree may be higher in the Jokhang Temple compared to the ones at low altitudes, probably due to the relatively lower oxygen level in the local air.

3.2.2. Concentration profile of the size-resolved PAHs

The individual PAH concentration in PM on average is shown in Fig. 3. The total concentration of PAHs was estimated as being 331.2 ± 60.3 ng/m^3. BaA (179.5 ± 15.2 ng/m^3) was the most abundant component, followed by Chry (30.6 ± 11.0 ng/m^3), BaP (18.6 ± 7.7 ng/m^3), NaP (15.8 ± 5.5 ng/m^3), FL (14.0 ± 4.5 ng/m^3), Acy (12.0 ± 2.6 ng/m^3), BkF (11.3 ± 3.6 ng/m^3), BbF (10.7 ± 3.8 ng/

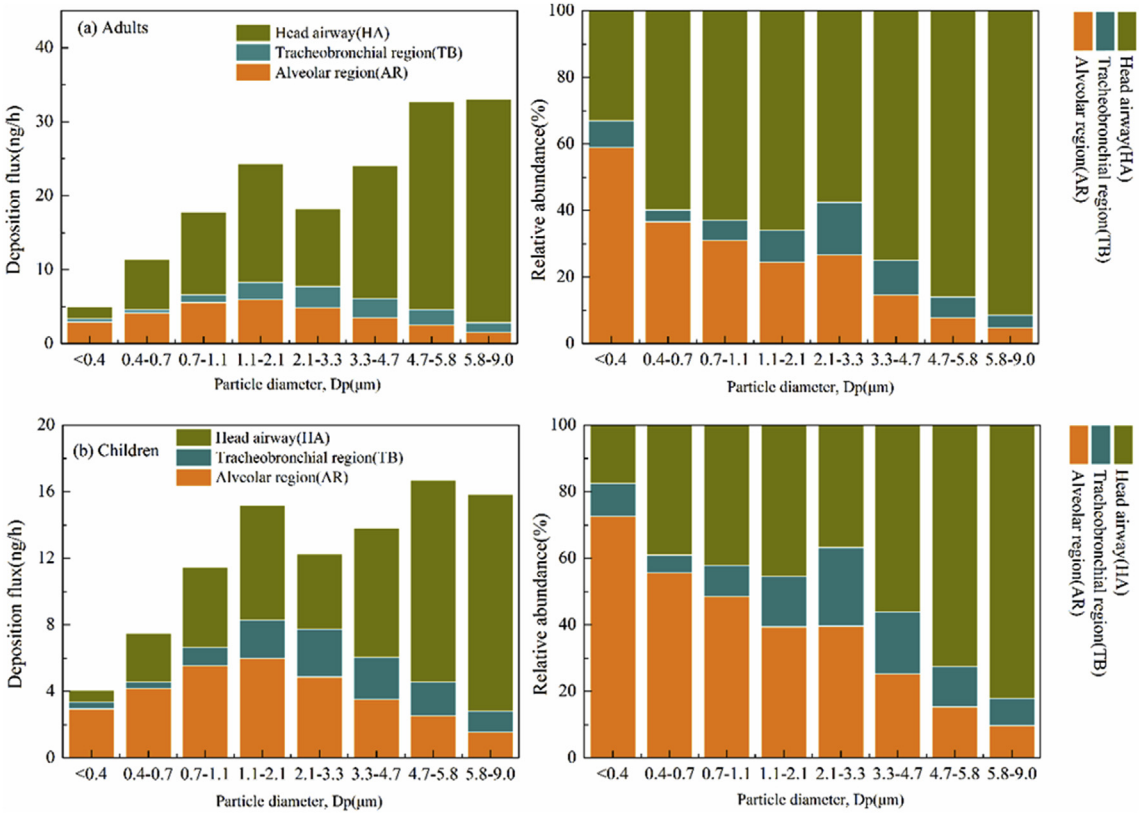

Fig. 6. Deposition flux of the size-resolved PAHs in the human respiratory tract and relative deposition flux in the head airway, tracheobronchial region, and alveolar region.

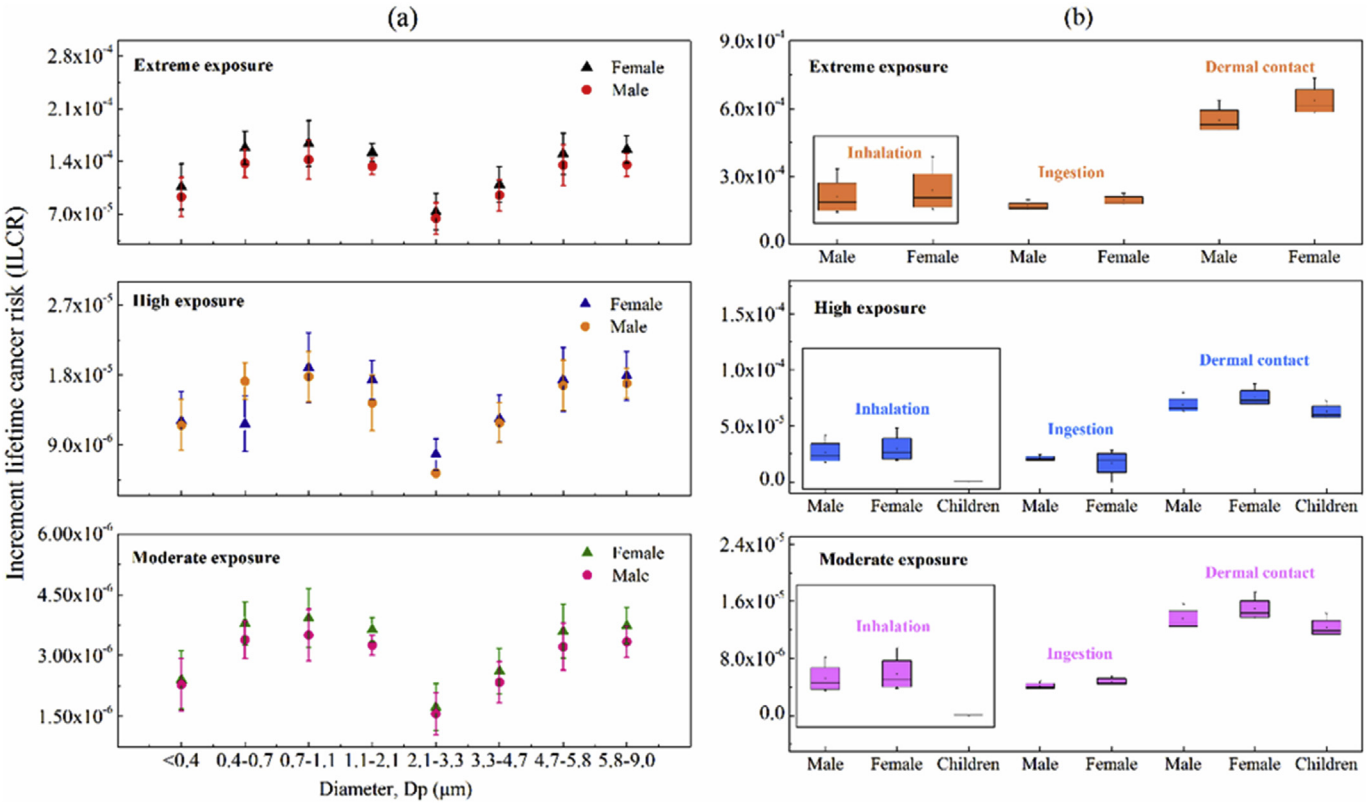

Fig. 7. Health risk assessment of PAHs. (a): ILCR due to exposure to the size-resolved PAHs. (b): cancer risk assessment of PAHs for the extreme, high and moderate exposure groups.

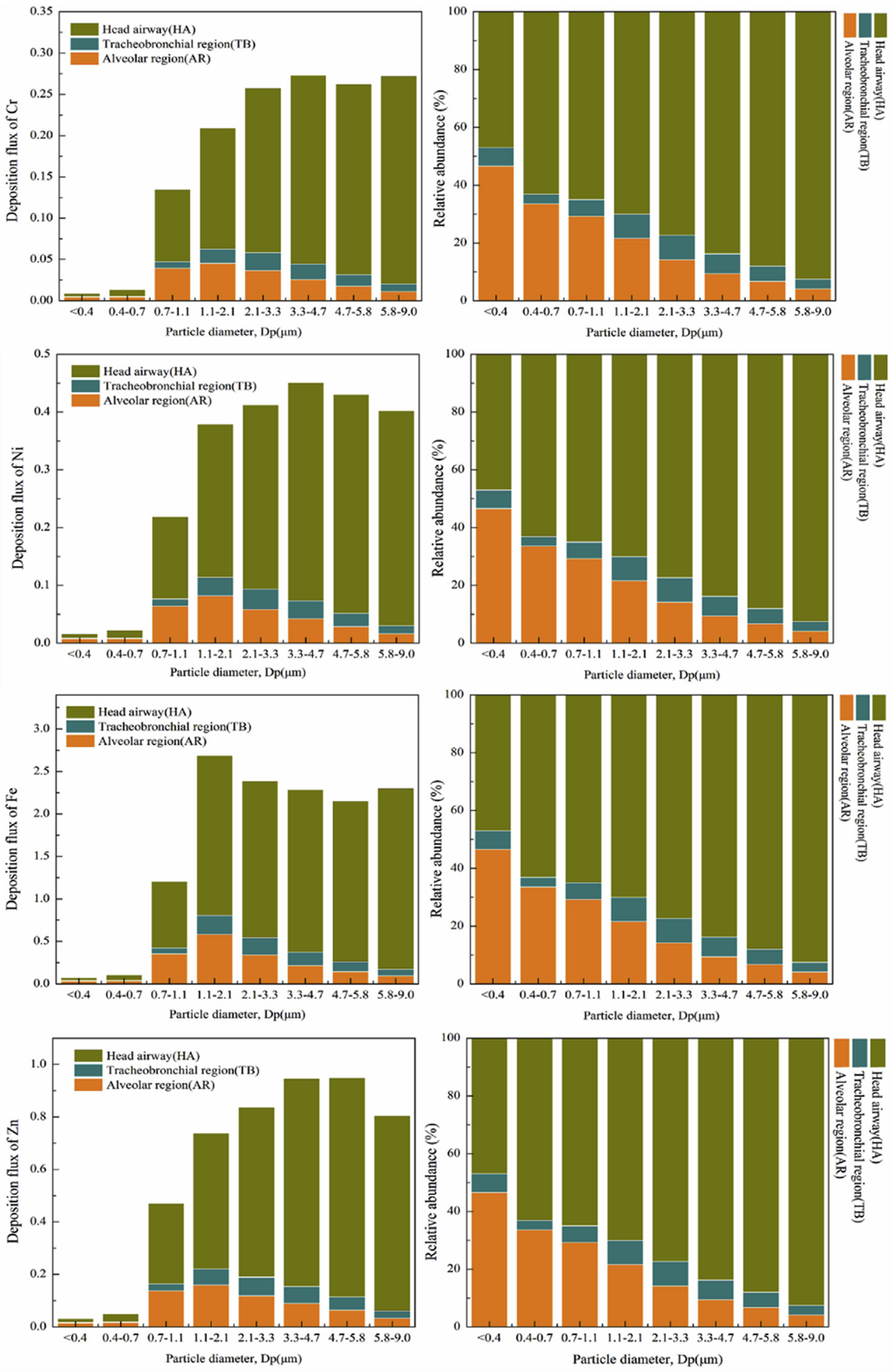

Fig. 8. Deposition flux of the size-resolved metals in the human respiratory tract and relative metals abundance of in the head airway, tracheobronchial region, and alveolar region.

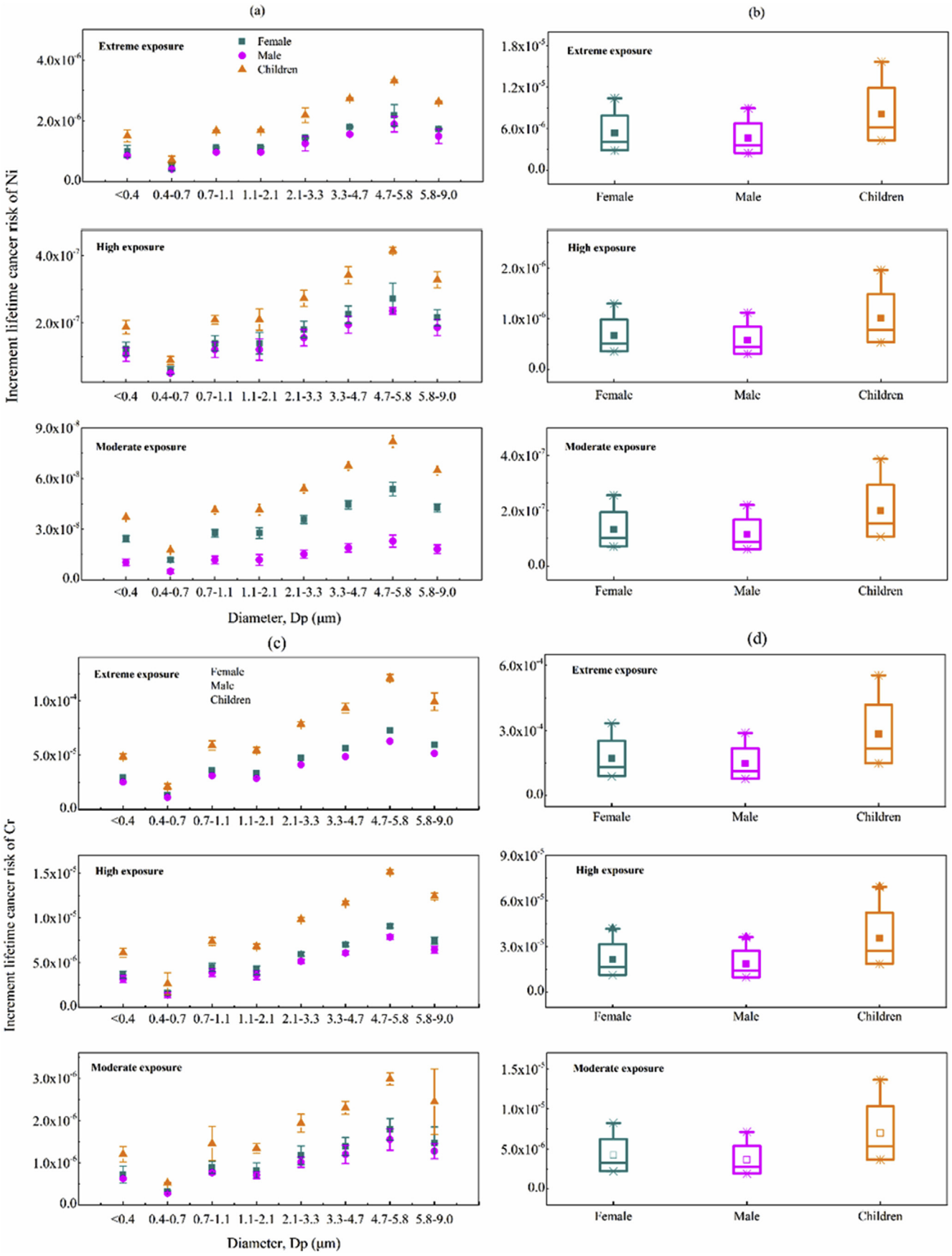

Fig. 9. Health risk assessment of Ni and Cr (a): ILCR of Ni due to exposure to the size-resolved PM. (b): cancer risk assessment of Ni for the extreme, high and moderate exposure groups, respectively. (c): ILCR of Ni due to exposure to the size-resolved PM. (d): cancer risk assessment of Cr for the extreme, high and moderate exposure groups, respectively.

m^3), Ace (10.5 ± 4.5 ng/m^3), Phe (4.3 ± 2.1 ng/m^3), Ant (4.2 ± 2.0 ng/m^3) and Flu (1.7 ± 1.1 ng/m^3). With regard to the number distribution of aromatic ring, both five-ring and four-ring were dominant, which accounted for 74.8% and 7.7% of the total PAHs by mass, respectively. It was well known that most high molecular-weight PAHs were mutagenic and/or carcinogenic, likely to threaten human health (Kameda et al., 2005).

To describe the size distribution of PAH, the $dC/dlogD_p$ was plotted as a function of D_p in Fig. 4. Most of PAH species (NaP, Acy, Ace, Flo, Phe, Ant, BkF, BbF, BaP) showed the trimodal size distributions, with two peaks in the fine mode and one peak in the coarse mode. Along with the increase of aromatic rings, the peak intensities varied, and the fine mode peak intensity increased in the high-molecular PAH species (BkF, BaP, BbF). Wu et al. (2006) reported that PAHs with high molecular-weight showed a tendency of accumulating in the fine particles, which could be attributed to that high-molecular PAHs are less volatile, and thus preferentially condense onto fine PM. In contrast, the low-molecular PAH species are more volatile, and are thus inhibited on finer particles as a consequence of the Kelvin effect (Dewangan et al., 2014; Hien et al., 2007; Andrea et al., 2016).

3.2.3. Concentration profiles of size-resolved metals

The elemental concentration profile was dominated by Na, Ca, Al, Mg and K (Fig. 5), of which the mean concentrations were 226.6, 82.2, 61.5, 38.4 and 28.5 ng/m^3, respectively. The principal metallic components detected in PM closely resembled those detected in the wood ash, as reported by Lin et al. (2007). Other species, including Fe, Sr, Zn, P, Ni and Cr, were detected in the smaller concentrations of 3.0, 2.5, 2.2, 1.3, 1.1 and 0.6 ng/m^3, respectively.

The elemental size distributions are shown in Fig. S2. One can see that the elements clearly showed a bimodal distribution with peaks in the size bins of 0.7–1.1 and 4.7–5.8 μm, respectively. The peak in the fine mode might be ascribed to condensation of vapor during the combustion process, whereas the peak in the coarse fraction could be attributed to the incomplete combustion, and/or resuspension of ground dust due to pilgrim's walking (Mannix et al., 1996; Li et al., 2017a,b). It was well documented that the mass concentrations of particulate metals inside the temples at low altitude were mainly concentrated in the fine mode (Fang et al., 2003; Hsueh et al., 2012). In contrast, a relatively larger proportion of the metal mass was distributed in the coarse mode in the present study. The significant different mass profiles herein could be associated with incomplete combustion of metals due to their high melting points, and insufficient oxygen level in the atmosphere of Tibet Plateau.

3.3. Health implications of the PM collected from the Jokhang Temple

3.3.1. Health risk of size-resolved PAHs

Intake of PAHs hosted by particles is associated with an excess risk of lung cancer (Grimmer et al., 1988). Especially, BaP was listed as Group 1 level carcinogen (IARC, http://www.iarc.fr/), and ranked 8th of 275 priority listed hazardous substances (ATSDR, 2011). The mean BaP concentration measured in the Jokhang Temple was 18.5 ng/m^3, which was much higher by ten times than the maximum permissible risk value of 1 ng/m^3 on account of carcinogenic potency of particulate PAHs through inhalation (Slooff et al., 1989). The BaP equivalent concentration (BaPeq) was generally used to evaluate the carcinogenic potency of the multi-component PAH exposure, which was calculated by multiplying the concentration of individual PAH and its toxic equivalent factor (TEF) given by Nisbet and LaGoy (1992). TEF of the individual PAH is listed in Table S3. The calculated BaPeq concentration was 40.9 ng/m^3, which was four times higher than the daily BaPeq standard of 10 ng/m^3 of the United State Environmental Protection Agency's (US-EPA, 1996). Therefore, it is likely that PAHs exposure in the Jokhang Temple could exert health hazards to human. To further evaluate the human risk of PAHs collected from the Jokhang Temple indoors, the respiratory exposure to size-resolved PAHs was assessed, and the health risk via inhalation, ingestion and dermal contact was calculated.

For evaluating the respiratory exposure, the deposition efficiency of size-resolved PAHs was incorporated. As shown in Fig. S3, the deposition efficiency increased with the particle size increase except for the alveolar region, in which the deposition efficiency decreased with the increase of particle size. Coarse particles made a greater contribution in the head region as compared to the alveolar and tracheobronchial region, probably due to that the coarse particles could be inhabited by the nasal area, and thus they had a less chance of reaching the alveolar and tracheobronchial region (Lyu et al., 2017). In contrast, finer particles could pass the respiratory tract easily and deposit in the alveolar region. Such phenomenon, combined with the fact that most of the high-molecular weight (four and five ring) PAHs tend to absorb in finer particles, makes them more important for potential human damage.

Fig. 6 shows the deposition fluxes of the size-resolved PAHs and their relative contributions in the head, tracheobronchial, and alveolar region. The highest total deposition flux occurred in the head region (73.6%), followed by the alveolar (18.7%) and tracheobronchial region (7.7%). The deposition flux was bimodal with peaks in the size range of 1.1–2.1 and 4.7–5.8 μm, respectively. The total PAH deposition flux was 123.6 ng/h for adults, which was much higher than that obtained in the urban community of Guangzhou (3.7 ng/h) (Zhang et al., 2012), but was much lower than that for traffic police exposure to vehicles emission in Beijing (280 ng/h) (Liu et al., 2007). Moreover, the deposition flux level varied among the different particle sizes. When particle size increased, the deposition flux increased in the head region, but decreased in the alveolar region, suggesting that coarse particles contributed most PAHs deposition in the head region, while fine particles contributed most PAHs in the alveolar region. The fine particles could pass rapidly from the human lung into the circulatory system, causing systematic exposure to PAHs (Nemmar et al., 2002).

Fig. 7 shows the cancer risk assessment of PAHs under extreme, high and moderate exposure conditions, respectively. As shown in Fig. 8a, the ILCR value exhibited two peaks with the higher one in the fine mode, whereas the lower one in the coarse mode, which was consistent with the distribution pattern of deposition flux. Specifically, fine mode PAHs contributed about 53.7% of the total ILCR, suggesting that the majority of cancer risk could be caused by the fractions of PAHs hosted by fine PM. Among three exposure routes (inhalation, ingestion and dermal contact), dermal contact posed the highest cancer risk to human, followed by inhalation and ingestion pathways, respectively. PAHs exerted higher cancer risk to female, then to male and lastly to children. For the extreme exposure to carcinogenic PAH inside the temple, the integrated ILCR values were 3.9×10^{-4} and 4.3×10^{-4} for male and female, respectively. For the high exposure group, the ILCR values were 1.2×10^{-4} for female, 1.2×10^{-4} for male, and 6.3×10^{-5} children, respectively. The ILCR values for moderate exposure group (female: 2.6×10^{-5}; male: 2.2×10^{-5}; children: 1.3×10^{-5}) were much lower than those for the high exposure group, but still exceeded the acceptable level of 10^{-6}. The data shown herein suggested that PAHs posed high or potential health risk to both adults and children.

The ILCR value of PAHs obtained herein was significantly lower than that estimated in the temples in Taiwan (Chiang et al., 2009)

and Thailand (Susira et al., 2016). The health risks implicated with worship could be related to the amount of incense burned, and/or the emission efficiency of the PAHs species, depending on incense type, combustion condition and environmental factors (Englert, 2004). Based on the ILCR value through three exposure routes, the visiting frequencies for temple visitors were recommended to be 41, 23 and 21/year for children, adult male and female, respectively.

3.3.2. Health risk of size-resolved metals

For the metallic elements hosted within the particles, Cr, Ni, Fe and Zn could be potentially risk to human body, all of which could be immediately internalized (Adamson et al., 2000), exerting the adverse effects to human health. Carcinogenic Cr and Ni harbor the potential to catalyze ROS formation.

The deposition fluxes of the size-resolved metals are shown in Fig. 8. The total deposition flux of metals was estimated at 1.4–13.2 ng/h. The main contributor to the total deposition flux occurred in the head region (80.9%), followed by the alveolar region (12.9%), and the tracheobronchial region (6.2%). The high deposition flux of the metals in the head region was attributed to the combined effects of three deposition mechanisms concluding diffusion, impaction and sedimentation (Lippmann, 2011). The deposition flux nearly showed a unimodal distribution pattern with one peak in the coarse mode, and coarse particles contributed to about 69.1%–74.4% of the total deposition flux value on average. Along with the increase of particle size, the deposition flux in the head region increased. The large particles (>2 μm) tend to deposit in the head region because of the filtering effect of nose (Oberdorster, 2004). Among the deposited particles, most of them could be expelled by sneezing or wiping (Nagar et al., 2014), leaving only a small amount of particles in the head region. In spite of that, the residual particles still could pose adverse health effects to human (e.g. nasal dysfunction) (Seilkop and Oller, 2003). It was well documented that some particle-bound metals including Ni and Zn could cross synapses in the olfactory bulb from nasal cavity area and migrate to distant nuclei of the brain via secondary olfactory neurons (Sunderman, 2001).

The carcinogenic risks of Ni and Cr are shown in Fig. 9, and non-cancer risks of Fe and Zn are shown in Figs. S4 and S5, respectively. Both ILCR and HQ exhibited a unimodal distribution with the peak in the size range of 4.7–5.8 μm. On average, coarse mode metals contributed about 66.5% of ILCR and 66.3% of HQ, respectively, suggesting that coarse particles were major harmful metal carriers. A significant elevation of both ILCR and HQ for children was observed, indicating the higher risks for children than adults. As shown in Tables S4 and S5, the main risk for human is originated from ingestion, followed by dermal contact, and inhalation. The particles that adhere to human hands might enter human body through an unconscious hand-to-month contact behaviors (Lyu et al., 2017). On the other hand, limited quantity of the metals hosted by particles could be inhaled into the respiratory system, because the metal mass concentration were mainly distributed in the coarse mode. In addition, the lower body weight of children is propitious to ingest greater quantity of particle-contaminated substances than adults (Beamer et al., 2008).

The integrated HQ values of Fe and Zn via three contact routes ranged between 10^{-5}-10^{-4} and 10^{-6}-10^{-5}, respectively, which were much lower than the safe level of 1.0, indicating non-cancer risks from the three exposure routes for Fe and Zn. In the case of the extreme exposure group, the integrated ILCR value of Cr was 4.9×10^{-5}, and for the high exposure and moderate exposure groups, the estimated ILCR values of Cr were 6.1×10^{-6} and 1.2×10^{-6}, respectively, indicating a potential cancer risk of Cr exposure to human. The integrated ILCR value of Ni for the extreme exposure group was 1.5×10^{-6}, while that for the high and moderate exposure group were lower than 10^{-6}. The cancer risk of two carcinogenic metals in the particles collected from the Jokahng Temple was much lower than that in the Taiwanese temples (Lin and Shen, 2003). However, the health risk of metals in the Jokhang Temple should not be overlooked in view of the higher ILCR values than those of the guidelines.

3.4. Uncertaintiesand limitations of health risk assessment

The health risk assessment of PAHs andtrace metals conducted by mathematical models could be influenced by somelimitations in our data sources, especially the inherent problem of uncertaintyand variability of the data. Firstly, the exposure factors and toxic parameterswere directly adopted from public and regulatoryauthority's guideline values, due to the lack of such reference values in China (Shiet et al., 2011). This may be infeasible for the actualevaluation of local populations. Secondly,the study lacks a long term monitoring of PAH and metals in the templeindoors, which may be considered as a limitation of the study due toconstraints from temple management to conduct such longitudinal studies. Weassume that the particle emissions could be much higher than that observed inthis study during special occasions such as World Incense Day of Tibetan and GreatPrayer Festival etc. Despite of the uncertainties and limitations, the modeladopted in this study captures the essential risk analysis methodology and isflexible enough to integrate effects occurring at varying subpopulation scales.

4. Conclusions

The physicochemical properties of incense burning PM in the Jokhang Temple indoors, as well as the implication to human health were determined in this study. The mean concentrations of $PM_{1.0}$ and $PM_{2.5}$ reached at 435 ± 309.5 and 483 ± 284.9 μg/m^3, respectively. The $PM_{2.5}$ mass concentration exceeded the National Ambient Air Quality Standard (NAAQS, 75 μg/m^3) by 6.4 times. The aerosol size showed a bimodal distribution with one peak in the fine mode (0.4–0.7 μm) and the other peak in the coarse mode (4.7–5.8 μm). Specifically, the mass fraction of coarse particles was 41.1%, apparently higher than that observed at low altitudes, probably due to the hypoxic atmospheric environment at Tibet Plateau. The total concentration of PAHs was 331.2 ± 60.3 ng/m^3, and the BaP concentration (18.5 ng/m^3) was over ten times higher than the maximum permissible risk value of 1 ng/m^3 on account of carcinogenic potency of particulate PAHs through inhalation. PAHs exhibited a trimodal distribution with two peaks in the fine mode and one peak in the coarse mode. Metals exhibited a bimodal size distribution with a dominant peak in the coarse mode. ILCR of PAHs was estimated as being 10^{-5}-10^{-4}, indicated high health risk to temple goers/workers. PAHs in fine mode contributed about 53.7% of the total ILCR. The highest ILCR of Cr and Ni were 5.5×10^{-5} and 1.5×10^{-6}, respectively, exceeding the cancer risk guideline (10^{-6}). HQ of Fe (10^{-5}-10^{-4}) and Zn (10^{-6}-10^{-5}) were much lower than the safe level of 1.0. Coarse mode metals contributed about 66.5% of ILCR and 66.3% of HQ on average, respectively indicating that coarse particles were major harmful metal carriers.

The data shown herein suggested that incense burning in the Jokhang Temple could emit massive quantities of primary PM hosting a complex mixture of hazardous compounds, which could substantially deteriorate the temple indoor air quality, and exert adverse effects to human health. Our finding highlights the necessity for further research in this unique region, and establishing public policies on the health risks associated with the religious tradition at Lhasa, Tibet Plateau.

Acknowledgments

This work was supported by National Key R&D Program of China (2016YFC0202700), Ministry of Science and Technology of China (2016YFE0112200), National Natural Science Foundation of China (Nos. 91744205, 21777025, 21577022, 21190053, 40975074), Marie Skłodowska-Curie Actions (690958 - MARSU-RISE - 2015) and International cooperation project of Shanghai municipal government (15520711200).

Appendix A. Supplementary data

Supplementary data related to this article can be found at https://doi.org/10.1016/j.envpol.2017.10.107.

References

Adamso, I.Y.R., Prieditis, H., Hedgecock, C., Vincent, R., 2000. Toxicol. Appl. Pharmacol. 166, 111–119.
Agency for Toxic Substances and Disease Registry (ATSDR), 2011. Toxic Substances Portal (CAS #84145-82-4, 14797-65-0) (Atlanta, GA, USA).
Andrea, Cattaneo, Paola, Fermo, Patrizia, Urso, Maria Grazia, Perrone, Andrea, Piazzalunga, Jessica, TarlassiP., aolo, Carrer, Domenico, Maria Cavallo, 2016. Particulate-bound polycyclic aromatic hydrocarbon sources and determinants in residential homes. Environ. Pollut. 218, 16–25.
Beamer, P., Key, M.E., Ferguson, A.C., Canales, R.A., Auyeung, W., Leckie, J.O., 2008. Quantified activity pattern data from 6 to 27-month-old farmworker children for use in exposure assessment. Environ. Res. 108, 239–246.
Beko, G., Weschler, C.J., Langer, S., Callesen, M., Toftum, J., Clausen, G., 2013. Total phthalate intakes estimated from urine of Danish children: comparisons with estimated intakes from dust ingestion, inhalation and dermal absorption in homes and daycare centers. PLoS One 8, 1–18.
Bitterle, E., Karg, E., Schroeppel, A., Kreyling, W.G., Tippe, A., Ferron, G.A., 2006. Dose-controlled exposure of A549 epithelial cells at the air–liquid interface to airborne ultrafine carbonaceous particles. Chemosphere 65, 1784–1790.
Susira, Bootdee, Somporn, Chantara, Tippawan, Prapamontol, 2016. Determination of $PM_{2.5}$ and polycyclic aromatic hydrocarbons from incense burning emission at shrine for health risk assessment. Atmos. Pollu. Res. 7, 680–689.
Chen, Y., Shah, N., Braun, A., Huggins, F.E., Huffman, G.P., 2005. Electron microscopy investigation of carbonaceous particulate matter generated by combustion of fossil fuels. Energy Fuel 19, 1644–1651.
Cheng, X., Huang, Y., Long, Z.J., Ni, S.J., Shi, Z.M., Zhang, C.J., 2016. Characteristics, sources and health risk assessment of trace metals in PM_{10} in Panzhihua, China. Bull. Environ. Contam. Toxicol. https://doi.org/10.1007/s00128-016-1979-0.
Chiang, K.C., Chio, C.P., Chiang, Y.H., Liao, C.M., 2009. Assessing hazardous risks of human exposure to temple airborne polycyclic aromatic hydrocarbons. J. Hazard. Mater 166, 676–685.
Delgado-Saborit, J.M., Aquilina, N., Meddings, C., Baker, S., Harrison, R.M., 2009. Measurement of personal exposure to volatile organic compounds and particle associated PAH in three UK regions. Environ. Sci. Technol. 43, 4582–4588.
Delgado-Saborit, J.M., Aquilina, N., Baker, S., Harrad, S., Meddings, C., Harrison, R.M., 2010. Determination of atmospheric particulate-phase polycyclic aromatic hydrocarbons from low volume air samples. Anal. Methods 2, 231–242.
Dewangan, S., Pervez, S., Chakrabarty, R., Zielinska, B., 2014. Uncharted source of particle bound polycyclic aromatic hydrocarbons from South Asia: religious ritual burning practices. Atmos. Pollut. Res. 5, 283–291.
Englert, N., 2004. Fine particles and human health-a review of epidemiological studies. Toxicol. Lett. 149, 235–242.
Fang, G.C., Chang, C.N., Chu, C.C., Wu, Y.S., Fu, P.C., Chang, S.C., Yang, I.L., 2003. Fine ($PM_{2.5}$), coarse ($PM_{2.5-10}$), and metallic elements of suspended particulates for incense burning at Tzu Yun Yen temple in central Taiwan. Chemosphere 51, 983–991.
Fang, G.C., Lin, S.J., Lee, J.F., Chang, C.C., 2009. A study of particulates and metallic element concentrations in temple. Toxicol. Ind. Health 25, 93–100.
Fang, W., Yang, Y., Xu, Z., 2013. PM_{10} and $PM_{2.5}$ and health risk assessment for heavy metals in a typical factory for cathode ray tube television recycling. Environ. Sci. Technol. 47, 12469–12476.
Gong, P., Wang, X.P., Yao, T.D., 2011. Ambient distribution of particulate and gas phase n-alkanes and polycyclic aromatic hydrocarbons in the Tibetan Plateau. Environ. Earth Sci. 64, 1703–1711.
Grimmer, G., Brune, H., Dettbarn, G., Naujack, K.-W., Mohr, U., Wenzel-Hartung, R., 1988. Contribution of polycyclic aromatic compounds to the carcinogenicity of sidestream smoke of cigarettes evaluated by implantation into the lungs of rats. Cancer Lett. 43, 173–177.
Heinrich, U., Roller, M., Pott, F., 1994. Estimation of a lifetime unit lung cancer risk for benzo (a) pyrene based on tumour rates in rats exposed to coal tar/pitch condensation aerosol. Toxicol. Lett. 72, 155–161.
Hien, T.T., Thanh, L.T., Kameda, T., Takenaka, N., Bandow, H., 2007. Distribution characteristics of polycyclic aromatic hydrocarbons with particle size in urban aerosols at the roadside in Ho Chi Minh City, Vietnam. Atmos. Environ. 41, 1575–1586.
Hsueh, H.T., Ko, T.H., Chou, W.C., Hung, W.C., Chu, H., 2012. Health risk of aerosols and toxic metals from incense and joss paper burning. Environ. Chem. Lett. 10, 79–87. https://doi.org/10.1007/s10311-011-0331-5.
Hussein, T., 2014. Particle size distributions inside a university office in Amman, Jordan. Jordan J. Phys. 7, 73–83.
Jetter, J.J., Guo, Z., McBrian, J.A., Flynn, M.R., 2002. Characterization of emissions from burning incense. Sci. Total Environ. 295, 51–67.
Jiang, Y., Jingke, S.I.M.A., Zhao, L., 2016. Bioaccessibility and health risk of heavy metals in particulate matters from residential and industrial areas in Shanghai. China. Environ. Chem. 35 (7), 1337–1345.
Jones, A.P., 1999. Indoor air quality and health. Atmos. Environ. 33, 4535–4564.
Kameda, Y., Shirai, J., Komai, T., Nakanishi, J., Masunaga, S., 2005. Atmospheric polycyclic aromatic hydrocarbons: size distribution, estimation of their risk and their depositions to the human respiratory tract. Sci. Total Environ. 340, 71–80.
Karimatu, L., Abdullahi, Delgado-Saborit, Juana Maria, Harrison, Roy M., 2013. Emissions and indoor concentrations of particulate matter and its specific chemical components from cooking: a review. Atmos. Environ. 71, 260–294.
Kawanaka, Y., Matsumoto, E., Sakamoto, K., Wang, N., Yun, S.J., 2004. Size distributions of mutagenic compounds and mutagenicity in atmospheric particulate matter collected with a low-pressure cascade impactor. Atmos. Environ. 38, 2125–2132.
Kuo, Su-Ching, Tsai, Ying I., 2017. Emission characteristics of allergenic terpenols in PM2.5 released from incense burning and the effect of light on the emissions. Sci. Total. Environ. 584–585, 495–504.
Kuo, Chung-Yih, Yang, Y.H., Chao, M.R., Hu, Chiung-Wen, 2008. The exposure of temple workers to polycyclic aromatic hydrocarbons. Sci. Total Environ. 401, 44–50.
Li, C.L., Hu, Y.J., Chen, J.M., Ma, Z., Ye, X.N., Yang, X., Wang, L., Wang, X.M., Abdelwahid, Mellouki, Abdelwahid, Mellouki, 2015. Physiochemical properties of carbonaceous aerosol from agricultural residue burning: density, volatility, and hygroscopicity. Atmos. Environ. 140, 94–105.
Li, Z.S., Wen, Q.M., Zhang, R.L., 2017a. Sources, health effects and control strategies of indoor fine particulate matter ($PM_{2.5}$): a review. Sci. Total Environ. 1–13.
Li, R., Fu, H.B., Hu, Q.Q., Li, C.L., Zhang, L.W., Chen, J.M., Abdel, Wahid Mellouki, 2017b. Physiochemical characteristics of aerosol particles in the typical microenvironment of hospital in Shanghai, China. Sci. Total Environ. 580, 651–659.
Lin, T.S., Shen, F.M., 2003. Trace metals in Chinese joss stick smoke. Bull. Environ. Contam. Toxicol. 71, 135–141.
Lin, T.C., Chang, F.H., Hsieh, J.H., Chao, H.R., Chao, M.R., 2001. Characteristics of polycyclic aromatic hydrocarbons and total suspended particulate in indoor and outdoor atmosphere of a Taiwanese temple. Environ. Contam. Toxicol. 67, 332–338.
Lin, T.C., Chang, F.H., Hsieh, J.H., Chao, H.R., Chao, M.R., 2002. Characteristics of polycyclic aromatic hydrocarbons and total suspended particulate in indoor and outdoor atmosphere of a Taiwanese temple. J. Hazard. Mater 95, 1–12.
Lin, T.C., Yang, C.R., Chang, F.G., 2007. Burning characteristics and emission products related to metallic content in incense. J. Hazard. Mater 140, 165–172.
Lippmann, M., 2011. Regional deposition of particles in the human respiratory tract. Comp. Physiol. 213–232.
Liu, Y.N., Tao, S., Dou, H., Zhang, T.W., Zhang, X.L., Dawson, R., 2007. Exposure of traffic police to polycyclic aromatic hydrocarbons in Beijing, China. Chemosphere 66, 1922–1928.
Long, C.M., Suh, H.H., Catalano, P.J., Koutrakis, P., 2001. Environ. Sci. Technol. 35, 2089–2099.
Lung, S.C., Kao, M.C., 2003. Worshippers' exposure to particulate matter in two temples in Taiwan. J. Air & Waste Manage. 53 (2), 130–135.
Lyu, Y., Xu, T., Li, X., Cheng, T., Yang, X., Sun, X., Chen, J., 2016. Size distribution of particle-associated polybrominated diphenyl ethers (PBDEs) and their implications for health. Atmos. Meas. Tech. 9, 1025–1037.
Lyu, Y., Zhang, K., Chai, F.H., Cheng, T.T., Yang, Q., Zheng, Z.L., Li, X., 2017. Atmospheric size-resolved trace elements in a city affected by nonferrous metal smelting: indications of respiratory deposition and health risk. Environ. Pollu 224, 559–571.
Majestic, B.J., Schauer, J.J., Shafer, M.M., 2007. Aerosol. Sci. Technol. 41 (10), 925–933.
Mannix, R.C., Nguyen, K.P., Tan, E.W., Ho, E.E., Phalen, R.F., 1996. Physical characterization of incense aerosols. Sci. Total Environ. 193, 149–158.
Matura, M., Goossens, A., Bordalo, O., Garcia-Bravo, B., Magnusson, K., Wrangsjö, K., Karlberg, A.T., 2002. Oxidized citrus oil (R-limonene): a frequent skin sensitizer in Europe. J. Am. Acad. Dermatol 47, 709–714.
Morabia, A., Amstislavski, P.N., Mirer, F.E., Amstislavski, T.M., Eisl, H., Wolff, M.S., 2009. Air pollution and activity during transportation by car, subway, and walking. Am. J. Prev. Med. 37 (1), 72–77.
Nagar, J.K., Akolkar, A.B., Kumar, R., 2014. A review on airborne particulate matter and its sources, chemical composition and impact on human respiratory system. Int. J. Environ. Sci. 5, 447–463.
Nemmar, A., Hoet, P.H.M., Vanquickenborne, B., Dinsdale, D., Thomeer, M., Hoylaerts, M.F., Vanbilloen, H., Mortelmans, L., Nemery, B., 2002. Passage of inhaled particles into the blood circulation in humans. Circulation 105, 411–414.
Newman, M., 2010. Fundamentals of Ecotoxicology. CRC Press, Taylor and Francis group, Boca Raton, FL, USA.
Nisbet, C., LaGoy, P., 1992. Toxic equivalency factors (TEFs) for polycyclic aromatic hydrocarbons (PAHs). Regul. Toxicol. Pharm. 16, 290–300.

Oanh, N.T.K., Reutergardh, L.B., Dung, N.T., 1999. Emission of polycyclic aromatic hydrocarbons and particulate matter from domestic combustion of selected fuels. Environ. Sci. Technol. 33 (16), 2703–2709.
Oberdorster, G., 2004. Effects and fate of inhaled ultrafine particles. Nanotechnology and the environment (chapter 7). In: ACS Symposium Series, vol. 890. American Chemical Society Publications, pp. 37–59.
Pope, C.A., 1999. Mortality and air pollution: associations persist with continued advances in research methodology. Environ. Health Perspect. 107, 613–614.
Rasmussen, R.E., 1987. Mutagenic activity of incense smoke in salmonella typhimurium. B Environ. Contam. Tox 38, 827–833.
Rebecca, Cohen, Sexton, Kenneth G., Yeatts, Karin B., 2013. Hazard assessment of United Arab Emirates (UAE) incense smoke. Sci. Total Environ. 458–460, 176–186.
Schweizer, C., Edwards, R.D., Bayer-Oglesby, L., Gauderman, W.J., See, S.W., Wang, Y.H., Balasubramanian, R., 2007. Assessment of reactive oxygen species in combustion aerosols. Environ. Res. 103, 317–324.
Seilkop, S.K., Oller, A.R., 2003. Respiratory cancer risks associated with low-level nickel exposure: an integrated assessment based on animal, epidemiological and mechanistic data. Regul. Toxicol. Pharmacol. 37, 173–190.
Shih-Chun, Lung, Candice, Mei-Chung, Kao, 2003. Worshippers' exposure to particulate matter in two temples in Taiwan. J. Air & Waste Manage 53 (2), 130–135.
Shih-Chun, Candice, Lung, Hu, Shu-Chuan, 2006. Generation rates and emission factors of particulate matter and particle-bound polycyclic aromatic hydrocarbons of incense sticks. Chemosphere 50, 673–679.
Slooff, W., Janus, J.A., Matthijsen, A.J.C.M., Montizaan, G.K., Ros, J.P.M., 1989. Integrated Criteria Document PAHs. Report No. 758,474,011. The Netherlands National Institute of Public Health and Environmental Protection, Bilthoven.
Sunderman, F.W., 2001. Review: nasal toxicity, carcinogenicity, and olfactory uptake of metals. Ann. Clin. Lab. Sci. 31, 3–24.
Tsai, Y.I., Wu, P.L., Hsu, Y.T., Yang, C.R., 2010. Anhydrosugar and sugar alcohol organic markers associated with carboxylic acids in particulate matter from incense burning. Atmos. Environ. 44, 3708–3718.
US-EPA, 1996. Recommendations of the Technical Review Workgroup for Lead for an Approach to Assessing Risks Associated with Adult Exposures to Lead in Soil. United States Environmental Protection Agency, Washington DC.
US-EPA, 2001. Risk Assessment Guidance for Superfund: Volume III D Part a, Process for Conducting Probabilistic Risk Assessment. EPA 540-R-02e002. Office of Emergency and Remedial Response, Washington, DC.
Voutsa, D., Anthemidis, A., Giakisikli, G., Mitani, K., Besis, A., Tsolakidou, A., Samara, C., 2015. Size distribution of total and water-soluble fractions of particle-bound elementsdassessment of possible risks via inhalation. Environ. Sci. Pollut. Res. 22 (17), 13412–13426.
Wang, B., Lee, S., Ho, K., 2006. Chemical composition of fine particles from incense burning in a large environmental chamber. Atmos. Environ. 40, 7858–7868.
Wang, B., Lee, S., Ho, K., Kang, Y.M., 2007. Characteristics of emissions of air pollutants from burning of incense in temples, Hong Kong. Sci. Total Environ. 377, 52–60.
Wang, J.Z., Steven Sai Hang, H., Huang, R.J., Gao, M.L., Liu, S.X., Zhao, S.Y., Cao, J.J., Wang, G.H., Shen, Z.X., Han, Y.M., 2016. Characterization of parent and oxygenated-polycyclic aromatic hydrocarbons (PAHs) in Xi'an, China during heating period: an investigation of spatial distribution and transformation. Chemosphere 159, 367–377.
Weschler, C.J., 2006. Ozone's impact on public health: contributions from indoor exposures to ozone and products of ozone-initiated chemistry. Environ. Health Perspect. 114, 1489–1496.
Wierzbicka, A., Bohgard, M., Pagels, J.H., Dahl, A., Londahl, J., Hussein, T., Swietlicki, E., Gudmundsson, A., 2015. Quantification of differences between occupancy and total monitoring periods for better assessment of exposure to particles in indoor environments. Atmos. Environ. 106, 419–428.
Wu, S.P., Tao, S., Liu, W.X., 2006. Particle size distributions of polycyclic aromatic hydrocarbons in rural and urban atmosphere of Tianjin, China. Chemosphere 62, 357–367.
Yang, C.R., Lin, T.C., Chang, F.H., 2007. Particle size distribution and PAH concentrations of incense smoke in a combustion chamber. Environ. Pollut. 145, 606–615.
Zhang, K., Zhang, B.Z., Li, S.M., Wong, C.S., Zeng, E.Y., 2012. Calculated respiratory exposure to indoor size-fractioned polycyclic aromatic hydrocarbons in an urban environment. Sci. Total Environ. 431, 245–251.
Zheng, Z., Ma, J.H., 2013. Research on strengthening and innovating social management in Tibetan areas: taking temple management in Lhasa as an example. J. Ethnol. 17, 116–118.
Zhou, R., Yang, B., Wang, Y.H., 2016. Higher cytotoxicity and genotoxicity of cultivated versus natural agarwood incense smoke. Environ. Chem. Let. 14, 501–506.